

# CHEMISTRY OF MATERIALS

VOLUME 16, NUMBER 24

NOVEMBER 30, 2004

© Copyright 2004 by the American Chemical Society

## Communications

### Preparation of Silicalite-1 Micromembranes on Laser-Perforated Stainless Steel Sheets

Ester Mateo,<sup>†</sup> Ruth Lahoz,<sup>‡</sup>  
Germán F. de la Fuente,<sup>‡</sup> Andrés Paniagua,<sup>§</sup>  
Joaquín Coronas,<sup>\*,†</sup> and Jesús Santamaría<sup>†</sup>

Department of Chemical and Environmental  
Engineering, Institute of Materials Science of Aragón,  
CSIC, University of Zaragoza,  
50018 Zaragoza, Spain, and Department of  
Earth Sciences, University of Zaragoza,  
50009 Zaragoza, Spain

Received September 3, 2004

Revised Manuscript Received October 1, 2004

#### Introduction

During the past few years the field of applications of zeolite membranes has been extended from separations<sup>1,2</sup> to membrane reactors,<sup>3</sup> sensors,<sup>4,5</sup> and, very recently, to silicon-based microdevices.<sup>6,7</sup> In addition, many advances have been made in the preparation of high-quality zeolite membranes.<sup>8,9</sup> However, it is not yet

clear how some of the major obstacles that still remain in the path to their widespread industrial use can be circumvented. Among these are technical limitations (such as lack of stability and separation selectivity at high temperature) and their high estimated cost of approximately 2000 euros/m<sup>2</sup> per membrane module.<sup>10</sup> Because of this, the only industrial-scale application of zeolite membranes until now corresponds to the dehydration of solvents by pervaporation.<sup>11</sup> On the other hand, commercial applications of zeolite membranes do not necessarily imply dimensions of many square meters of permeation area in a single unit.<sup>3</sup> Actually, scaling-down should allow preparing true defect-free zeolite membranes (eventually single-crystal membranes) that would have a higher chance of tolerating the inherent thermal and mechanical stresses produced, for instance, during the calcination stage<sup>12</sup> or during thermal cycling. Zeolite micromembranes also would be able to perform the separation and reaction operations of standard zeolite membranes, while providing the following additional advantages: (i) easy integration, at the microscopic level, of reaction and separation; (ii) excellent temperature control; (iii) possible higher selectivity and conversion compared to conventional reactors; (iv) intrinsic safety; and (v) easier scale-up in a highly compact format. The latter four already have been quoted by

\* To whom correspondence should be addressed. E-mail: coronas@unizar.es.

<sup>†</sup> Department of Chemical and Environmental Engineering, University of Zaragoza.

<sup>‡</sup> Institute of Materials Science of Aragón.

<sup>§</sup> Department of Earth Sciences, University of Zaragoza.

(1) Tavoraro, A.; Drioli, E. *Adv. Mater.* **1999**, *11*, 975–996.

(2) Coronas, J.; Santamaría, J. *Sep. Purif. Methods* **1999**, *28*, 127–177.

(3) Coronas, J.; Santamaría, J. *Topic Catal.* **2004**, *29*, 29–44.

(4) Mintova, S.; Mo, S.; Bein, T. *Chem. Mater.* **2001**, *13*, 901–905.

(5) Vilaseca, M.; Coronas, J.; Cirera, A.; Cornet, A.; Morante, J. R.; Santamaría, J. *Catal. Today* **2003**, *82*, 179–185.

(6) Wan, Y. S. S.; Chau, J. L. H.; Gavrilidis, A.; Yeung, K. L. *Microporous Mesoporous Mater.* **2001**, *42*, 157–175.

(7) Chau, J. L. H.; Yeung, K. L. *Chem. Commun.* **2002**, 960–961.

(8) Hedlund, J.; Sterte, J.; Anthonis, M.; Bons, A. J.; Carstensen, B.; Corcoran, N.; Cox, D.; Deckman, H.; Gijnst, W. D.; de Moor, P. P.; Lai, F.; McHenry, J.; Mortier, W.; Reinoso, J.; Peters, J. *Microporous Mesoporous Mater.* **2002**, *52*, 179–189.

(9) Lai, Z.; Bonilla, G.; Díaz, I.; Nery, J. G.; Sujaoti, K.; Amat, M. A.; Kokkoli, E.; Terasaki, O.; Thompson, R. W.; Tsapatsis, M.; Vlachos, D. G. *Science* **2003**, *300*, 456–460.

(10) Meindersma, G. W.; de Haan, A. B. *Desalination* **2002**, *149*, 29–34.

(11) Morigami, Y.; Kondo, M.; Abe, J.; Kita, H.; Okamoto, K. *Sep. Purif. Technol.* **2001**, *25*, 251–260.

(12) Dong, J.; Lin, Y. S.; Hu, M. Z. C.; Peascoe, R. A.; Payzant, E. A. *Microporous Mesoporous Mater.* **2000**, *34*, 241–253.

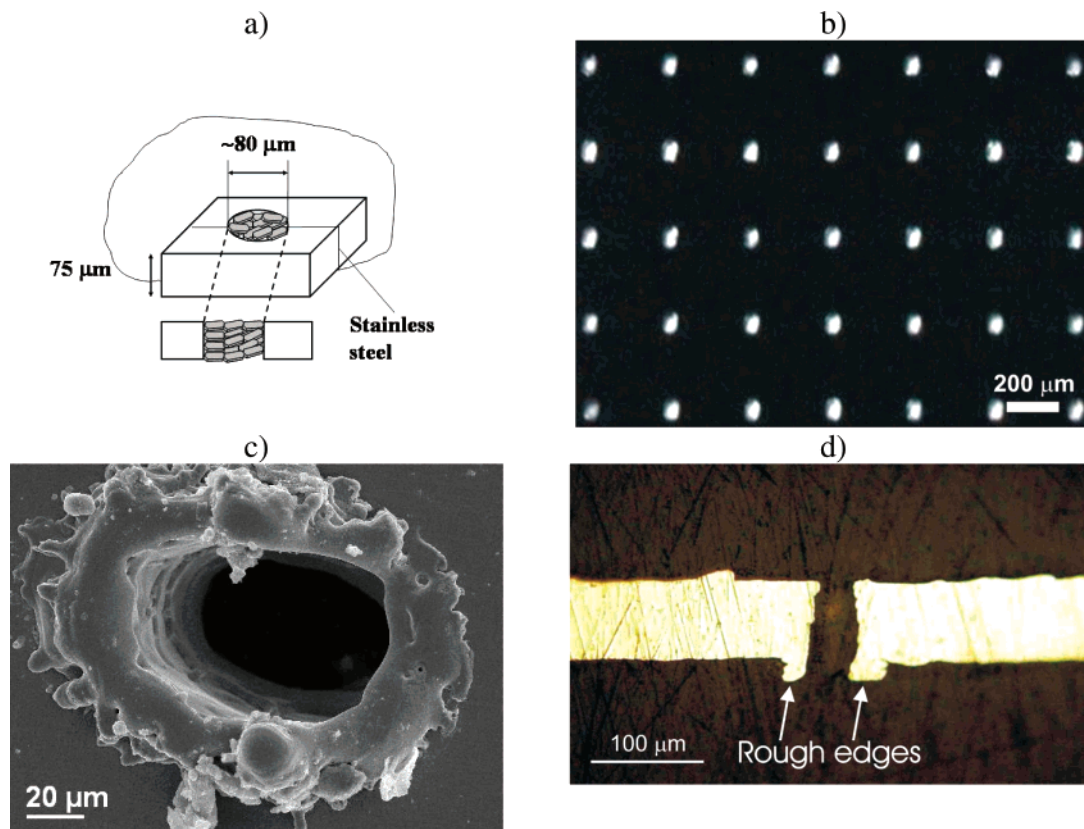


**Figure 1.** (a) Scheme of the zeolite micromembrane. Optical (b, d) and electronic (c) microscope images of a laser-perforated stainless steel sheet: (b) general view, (c) a hole with its rough edge in detail; and (d) cross section.

Kolb and Hessel<sup>13</sup> as general advantages of microreactors.

### Experimental Section

A 65-W, Q-switched Nd:YAG laser manufactured by Baasel Lasertech, emitting at a wavelength of 1064 nm in both continuous and pulsed mode, was used to perforate the 75- $\mu\text{m}$ -thick stainless steel sheets (5 Cr, 18 Ni, Record) and also to polish/remove the continuous zeolite layer prepared on the sheet. Perforation was achieved through ablation of the steel substrate, performed at a surface scan rate of 1500 mm/s, an average power of 4 W, a pulse repetition rate of 4.5 kHz, a pulse energy of 0.80 mJ, a fluence of 1.3 MJ/mm<sup>2</sup>, and a peak power of 3.14 GW/mm<sup>2</sup>. Laser polishing was achieved at an average power of 7 W, a pulse repetition rate of 20 kHz, a pulse energy of 0.35 mJ, a fluence of 0.80 MJ/mm<sup>2</sup>, and a peak power of 2.18 MW/mm<sup>2</sup>.

Silicalite-1 nanocrystals (ca. 100 nm) were obtained by hydrothermal synthesis at 100 °C for 18 h using a solution with the following molar composition: TPAOH/TEOS/H<sub>2</sub>O/EtOH = 9/25/408/100.<sup>14</sup> (TPA is tetrapropylammonium and TEOS is tetraethyl orthosilicate.) The gel was aged for 24 h. The nanoparticles were purified after synthesis by centrifugation until pH = 7 and then calcined at 480 °C for 8 h, with heating and cooling rates of 0.5 °C/min. The rough edges side of a laser-perforated stainless steel sheet (15 mm diameter) was seeded by rubbing with silicalite-1 nanocrystals. The support was

placed vertically in a Teflon-lined autoclave that was then filled with 20 mL of a solution having the following molar composition: KOH/TPABr/TEOS/H<sub>2</sub>O = 1/1/4.5/1000.<sup>15</sup> The hydrothermal synthesis (only one) took place at 170 °C for 24 h. Under these conditions the silicalite-1 crystals were produced mostly within the microholes and on the rough edges side of the support. The template was removed by calcinations at 480 °C for 8 h, with heating and cooling rates of 0.5 °C/min.

An array of micromembranes was placed and sealed by viton O-rings in a flat membrane module as if it were a 15-mm circular membrane. Mass flow controllers (Brooks Instruments B. V.) were used to feed continuously a 50 cm<sup>3</sup>(STP)/min stream of an equimolar mixture of propane and N<sub>2</sub> into the silicalite-1 membrane side (retentate), while the other side (permeate) was swept with a 25 cm<sup>3</sup>(STP)/min stream of Ar. The total pressure was maintained at atmospheric value on both sides of the membrane. Samples at the exit of both permeate and retentate streams were analyzed by on-line gas chromatography (CE Instrument 8000). The permeances were calculated using the log-mean partial pressure difference, and the separation factor as  $(y_{\text{propane}}/y_{\text{N}_2})/(x_{\text{propane}}/x_{\text{N}_2})$ , with  $y$  and  $x$  being the molar fractions in the permeate and retentate sides, respectively.

### Results and Discussion

A general scheme of the silicalite-1 micromembranes prepared in this work is given in Figure 1a. A set of

(13) Kolb, G.; Hessel, V. *Chem. Eng. J.* **2004**, *98*, 1–38.

(14) Mintova, S.; Valtchev, V.; Engström, V.; Schoeman, B. J.; Sterte, J. *Microporous Mater.* **1997**, *11*, 149–160.

(15) Xomeritakis, G.; Gouzinis, A.; Nair, S.; Okubo, T.; He, M.; Overney, R. M.; Tsapatsis, M. *Chem. Eng. Sci.* **1999**, *54*, 3521–3531.

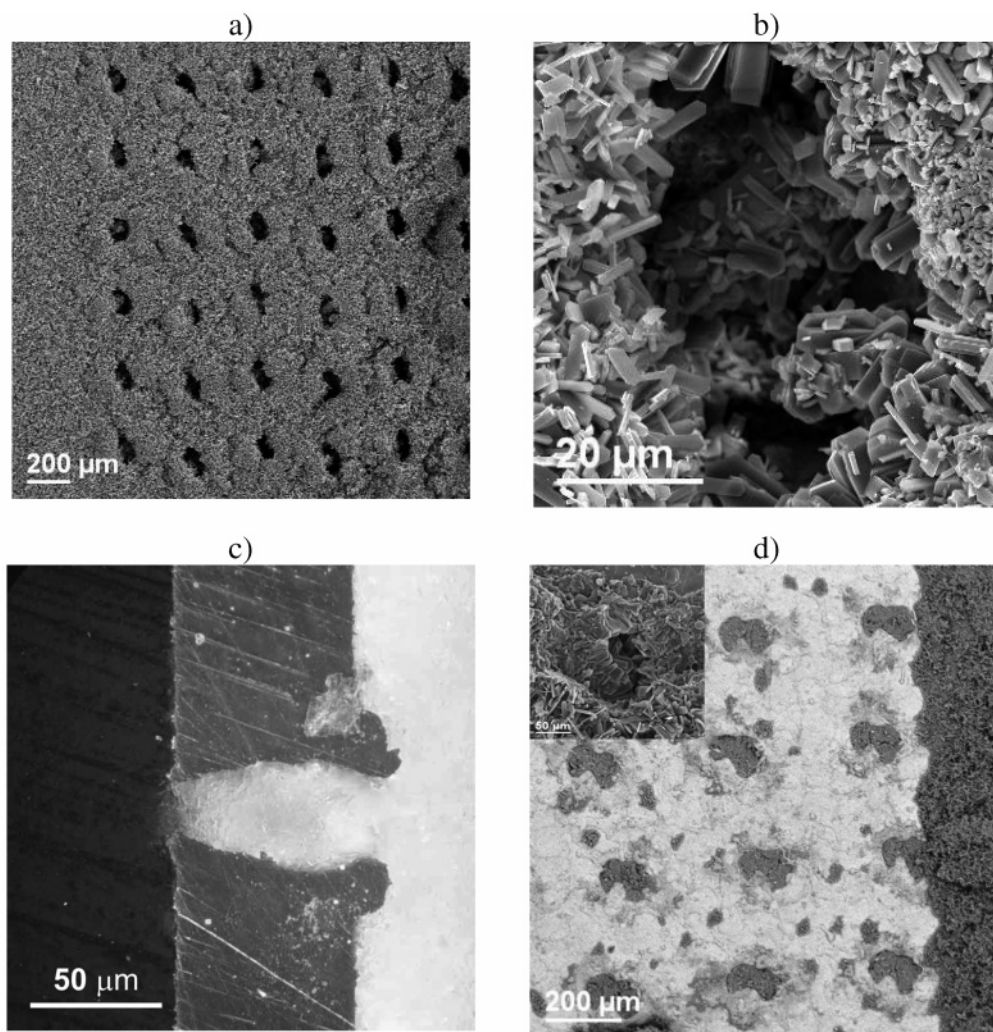


**Figure 2.** Electronic (a, b, d) and optical (c) microscope images: (a) general view of the plate surface after silicalite-1 synthesis, (b) top detailed view and (c) cross section of one of the zeolite-filled holes; (d) general view of the plate surface after laser polishing with detail of a microhole in the insert.

these membranes was prepared by using liquid phase hydrothermal synthesis to fill an array of approximately cylindrical holes of ca.  $80\text{-}\mu\text{m}$  inner diameter (i.e., with a free area of approximately  $0.005\text{ mm}^2$ ). Figure 1b shows an array of microholes before hydrothermal synthesis. The microholes were patterned on a  $75\text{-}\mu\text{m}$ -thick stainless steel sheet by a Nd:YAG laser to yield an array of  $364\text{ microholes/cm}^2$ . As can be seen in Figure 1c, where one of such microholes of ca.  $60 \times 90\text{ }\mu\text{m}$  is shown in detail, the laser-drilled holes are inherently associated with formation of rough edges due to the expulsion of molten steel from their inside. This process occurs typically when relatively long pulse widths ( $\tau$ ) are used in laser drilling, as is the case here with  $\tau = 0.4\text{ }\mu\text{s}$ , because heat transfer takes place efficiently onto the substrate's surface. A melt pool is thus formed at the focal spot, accompanied by the simultaneous appearance of a plasma which generates intense, localized shock waves in the direction of the substrate. These shock waves distribute the melt pool symmetrically around the focal spot and yield the rapidly solidified steel layers which are observed in the micrograph.<sup>16,17</sup>

Figure 1d is an optical microscope image of a cross section of a microhole, where it can be seen that the rough edges are  $10\text{--}15\text{ }\mu\text{m}$  high. Since the sample was embedded in resin to be polished and the polishing was difficult to stop just at the center of the perforation, the hole observed in Figure 1d has an apparent diameter smaller than that of the original laser perforation.

To prepare the silicalite-1 micromembranes, the perforated stainless steel plate was seeded using  $100\text{-nm}$  colloidal silicalite-1 particles that had been previously synthesized. Then the seeded plate was subjected to hydrothermal synthesis. XRD analysis was carried out in all the samples, showing that silicalite-1 was the only crystalline phase present in the micromembranes. The top view in Figure 2a shows that after synthesis the plate is almost totally covered by silicalite-1 crystals. The more detailed view in Figure 2b shows the characteristic shape of these crystals. The optical microscope image of Figure 2c indicates that silicalite-1 was synthesized along the whole perforation and also that all the exposed surface of the perforated sheet was covered with a continuous, ca.  $30\text{-}\mu\text{m}$ -thick layer of zeolite crystals. The thickness of this layer can be reduced by controlling the synthesis conditions, e.g. by lowering the temperature and/or the synthesis time. For instance, at

(16) Rubahn, H.-G. *Laser Applications in Surface Science and Technology*; Wiley: Chichester, 1999.

(17) Meijer, J. *J. Mater. Process. Technol.* **2004**, *149*, 2–17.



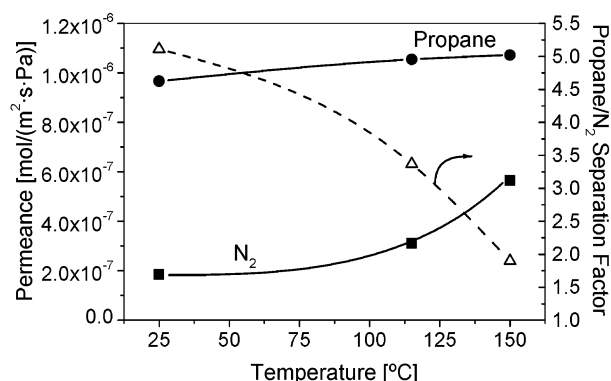


**Figure 3.** Separation of a 50/50 propane/N<sub>2</sub> mixture through a silicalite-1 micromembrane as a function of temperature.

100 °C and with a synthesis of the same duration (20 h), the thickness was reduced to only 1–2  $\mu\text{m}$  (not shown), while the perforations still appeared to be completely filled with silicalite-1 crystals. Unfortunately, at this moment such membranes do not have desirable permeation properties. On the other hand, the energy of the laser can also be employed to carefully remove the zeolite layer that is outside the holes. Figure 2d shows a general view of a laser-cleaned area. Apparently, the integrity of the micromembrane was not affected, as the hole remained filled with silicalite-1 crystals (Figure 2d, insert). However, removal of the outside zeolite layer that covers all the micromembranes reduced the resistance to permeation and the N<sub>2</sub> permeance at room temperature increased by an order of magnitude: from  $1.2 \cdot 10^{-7}$  to  $2.0 \cdot 10^{-6}$  mol/(m<sup>2</sup>·s·Pa).

To assess the performance of the as-prepared silicalite-1 micromembranes, they were used in the gas-phase separation of propane/N<sub>2</sub> mixtures. A propane/N<sub>2</sub> separation factor of 5.1 was found at room temperature (Figure 3) due to the preferential adsorption of propane on the zeolite pores, which hinders N<sub>2</sub> transport. This behavior, together with the temperature dependence of the permeances and selectivity, has been observed by several authors on silicalite-1 membranes when separating mixtures of light hydrocarbons (mostly *n*-butane) and permanent gases,<sup>2</sup> and is a good indication of the quality of the membranes prepared, as a significant presence of mesoporous defects would give selectivity

values close to the Knudsen level (1.3). As the temperature increases, propane adsorption decreases, and the separation factor was lowered to 1.9 at 150 °C. The propane permeance found in this work was above  $10^{-6}$  mol/(m<sup>2</sup>·s·Pa), a value much higher than the permeances usually reported for MFI-type zeolite membranes that tend to fall in the  $10^{-9}$ – $10^{-7}$  mol/(m<sup>2</sup>·s·Pa) range.<sup>18–20</sup> The high permeance of our silicalite-1 micromembranes can be attributed to the fact that they can be considered as self-supported, since the zeolite layer is in direct contact with both the feed and the permeate sides, while conventional zeolite membranes<sup>21</sup> are grown on thicker porous supports. In this case the transport resistance increases, as the permeating molecules diffuse through the support (and also through the zeolitic material that is often deposited in its pores).

### Conclusions

In summary, roughly circular silicalite-1 micromembranes with a diameter of ca. 80  $\mu\text{m}$  can be prepared on laser-perforated stainless steel sheets. An array of these micromembranes is able to separate the same kind of mixtures (e.g., propane and N<sub>2</sub>) as the common silicalite-1 membranes, at a much higher permeation flux. The main advantages of these micromembranes are (1) their self-supporting character, considering that the zeolitic material is in direct contact with both the feed and the permeate sides through a thickness of only 75  $\mu\text{m}$ ; (2) their reduced dimensions and high area-to-volume ratio that would facilitate withstanding the inherent stresses of thermal cycling; and (3) in general, the advantages quoted for microsystems in separation and reaction applications.

**Acknowledgment.** Financial support from DGA and CICYT, both in Spain, is gratefully acknowledged.

CM048504+

(18) Bakker, W. J. W.; van den Broeke, L. J. P.; Kapteijn, F.; Moulijn, J. A. *AIChE J.* **1997**, *43*, 2203–2214.

(19) Yang, M.; Crittenden, B. D.; Perera, S. P.; Moueddeb, H.; Dalmon, J. A. *J. Membr. Sci.* **1999**, *156*, 1–9.

(20) Bernal, M. P.; Coronas, J.; Menéndez, M.; Santamaría, J. *J. Membr. Sci.* **2002**, *195*, 125–138.

(21) Bernal, M. P.; Coronas, J.; Menéndez, M.; Santamaría, J. *Microporous Mesoporous Mater.* **2003**, *60*, 99–110.